AGU ADVANCING EARTH AND SPACE SCIENCES

Geophysical Research Letters

RESEARCH LETTER
10.1029/2025GL115382

Continental-Hemispheric Scale Dust Events Driven by Last Glacial Alpine Ice Sheet Dynamics

Yunus Baykal[1,2], Gábor Újvári[3,4], Thomas Stevens[1], Sergio Andò[5], Adriano Banak[6], Sanja Šuica[7], Marta Barbarano[5], and Eduardo Garzanti[5]

[1]Department of Earth Sciences, Uppsala University, Uppsala, Sweden, [2]Department of Physics, Technical University of Denmark, Roskilde, Denmark, [3]Institute for Geological and Geochemical Research, HUN-REN Research Centre for Astronomy and Earth Sciences, Eötvös Loránd Research Network, Budapest, Hungary, [4]CSFK, MTA Centre of Excellence, Budapest, Hungary, [5]Department of Earth and Environmental Sciences, University of Milano-Bicocca, Milano, Italy, [6]Department of Geology, Croatian Geological Survey, Zagreb, Croatia, [7]Department of Geology, University of Zagreb, Zagreb, Croatia

Key Points:

- Multi-proxy source study of detailed ^{14}C dated loess in Europe reveals Alpine Ice Sheet sediment supply drives last glacial dust events
- Wider dispersal of Alpine Ice Sheet dust potentially affected the North Atlantic region and amplified last glacial climate fluctuations
- Coherent explanation of millennial-scale dust-climate coupling during last glacial period

Supporting Information:

Supporting Information may be found in the online version of this article.

Correspondence to:

Y. Baykal,
yubay@dtu.dk

Citation:

Baykal, Y., Újvári, G., Stevens, T., Andò, S., Banak, A., Šuica, S., et al. (2025). Continental-hemispheric scale dust events driven by last glacial Alpine Ice Sheet dynamics. *Geophysical Research Letters*, *52*, e2025GL115382. https://doi.org/10.1029/2025GL115382

Received 17 FEB 2025
Accepted 27 MAY 2025

Author Contributions:

Conceptualization: Yunus Baykal, Gábor Újvári, Thomas Stevens, Sergio Andò, Eduardo Garzanti
Formal analysis: Yunus Baykal, Sergio Andò, Adriano Banak, Sanja Šuica, Marta Barbarano, Eduardo Garzanti
Investigation: Yunus Baykal, Gábor Újvári, Thomas Stevens, Sergio Andò, Adriano Banak, Sanja Šuica, Marta Barbarano, Eduardo Garzanti
Methodology: Yunus Baykal, Gábor Újvári, Thomas Stevens, Sergio Andò, Adriano Banak, Sanja Šuica, Marta Barbarano, Eduardo Garzanti
Visualization: Yunus Baykal
Writing – original draft: Yunus Baykal
Writing – review & editing: Gábor Újvári, Thomas Stevens,

Abstract

Greenland ice cores demonstrate that transient last glacial cold climate events (stadials) were associated with greatly enhanced atmospheric dust loading. Detailed radiocarbon dating of loess in central Europe reveals concurrent increases in dust activity in dust-emitting regions. However, the causes of these changes in dust emission and the role of dust in rapid climate change remain unclear. We address this uncertainty through multi-proxy analysis of loess sources in Hungary. Our results demonstrate that loess particles were dominantly produced by subglacial grinding processes in the eastern Alps. These particles were released along with stadial Alpine Ice Sheet-driven meltwater pulses, turning major river systems into efficient dust sources for loess deposition in Europe. Concurrent strengthened anticyclonic circulation over northern Europe would have caused wider dispersal of Alpine Ice Sheet-derived dust as far as Greenland. Resultant continental-hemispheric scale changes in atmospheric dust loading likely amplified concomitant North Atlantic climate cooling and ice sheet decay during Greenland stadials.

Plain Language Summary

Atmospheric dust is a fundamental component of Earth's climate system. Quaternary archives from dust-emitting and source distal regions reveal a close relationship between abrupt changes in dust and climate. However, the causes for this dust-climate coupling and the role of dust in rapid climate change events remain unclear. Here, we propose a mechanism that explains this coupling. Specifically, we show that last glacial dust in Central Europe was produced by subglacial grinding processes in the Alps. Alpine Ice Sheet recession events greatly enhanced proglacial sediment supply and turned major river systems into efficient but intermittent dust sources. Wider dispersal of Alpine Ice Sheet dust across the North Atlantic region likely amplified abrupt climate fluctuations during the last glacial.

1. Introduction

Rapid climate change events during the last glacial period (LGP) represent some of the most dramatic environmental shifts during the recent geological past. In particular, Greenland ice cores reveal that cold glacial climate was interrupted by numerous decadal-scale warming events of 5–16.5°C in amplitude (interstadials), followed by a more gradual, centennial-millennial scale return to colder conditions (stadials) (Kindler et al., 2014; Rasmussen et al., 2014). Across these abrupt climate transitions, Greenland ice cores record substantial changes in mineral dust content. In particular, dust particle concentrations were found to be dramatically increased during colder stadial periods with peak values during the Last Glacial Maximum (LGM: 26–19 ka; Clark et al., 2009), all demonstrating that climate variability during the LGP was associated with abrupt and substantial changes in the mineral dust cycle (Ruth et al., 2003). Atmospheric mineral dust interacts with climate through numerous feedbacks including radiative forcing, albedo and nutrient cycling (Bullard et al., 2016; Knippertz & Stuut, 2014). These feedbacks may be opposing and/or spatially variable, but the effective radiative impact of dust in the modern global atmosphere has been recently quantified to -0.2 ± 0.5 W m^{-2}, suggesting that dust net cools global climate (Kok et al., 2023). Dust also responds to climate change through changes in dust production, emission and transport (Knippertz & Stuut, 2014). However, the precise mechanisms behind the close coupling of dust and climate during the LGP are unclear and the role of dust in abrupt climate change remains elusive.

Sergio Andò, Adriano Banak, Sanja Šuica, Marta Barbarano, Eduardo Garzanti

Windblown mineral dust deposits (loess) in Europe serve as source-proximal dust archives and thus provide a means to study dust dynamics in the very regions where dust is produced (Figure 1a). Recent extremely detailed radiocarbon dating of last glacial loess deposition in the Middle Danube Basin, central Europe revealed phases of greatly enhanced dust activity matching the timing of stadial dust peaks in Greenland ice (Újvári et al., 2017). Moreover, dust provenance evidence suggests that central European dust sources potentially contributed to last glacial Greenland dust (Újvári et al., 2015, 2022), all raising the possibility that enhanced stadial dust emission from central Europe may have affected wider atmospheric dust loading across the North Atlantic region. However, understanding the causes of this dust deposition variability during the LGP is limited by uncertainties over the sources and origins of loess. For loess in the Middle Danube Basin, previously proposed contributions from distant dust sources such as North African deserts (Stuut et al., 2009; Varga et al., 2016) or Fennoscandian Ice Sheet outwash sediments (I. J. Smalley & Leach, 1978) are increasingly considered to be negligible (Baykal et al., 2021; Buggle et al., 2008; Fenn et al., 2025; Újvári et al., 2012). Instead, it is generally agreed that proximal floodplain sediments deposited by the Danube river and tributaries act as dominant source for loess deposition (Fenn et al., 2022; Pötter et al., 2021; Újvári et al., 2012). In contrast, the specific proto-sources for dust particle production prior to river transport, deflation and loess deposition remain debated.

Traditionally, the Alps and the Carpathians have been considered as proto-sources for loess in the Middle Danube Basin (Buggle et al., 2008; I. Smalley et al., 2009; Ujvári et al., 2012). However, other studies argue for the importance of smaller, more proximal mountain regions for sediment production, such as the Bohemian Massif (Újvári et al., 2013; Újvári & Klötzli, 2015), the Transdanubian Range (Thamó-Bozsó et al., 2014), or a combination of these (Fenn et al., 2022). Yet, identifying these ultimate production points of loess particles is essential for understanding the processes involved in dust production, their potential control on dust source activity and loess deposition, and the cause of the coupling to rapid climate change events. Specifically, while the Alps were covered with the extensive Alpine Ice Sheet (AIS) during the LGP (Seguinot et al., 2018), the presence of ice caps larger than isolated glacier lobes across other lower elevation mountain ranges surrounding the Middle Danube Basin is debated (Kłapyta et al., 2021; Mentlík et al., 2013; Urdea et al., 2011). Seasonal glacial melt of the last glacial AIS released large amounts of meltwater loaded with sub-glacially ground sediment particles into proglacial drainage systems of the Danube catchment. Moreover, study of Danube delta sediment accumulation rates and sources showed that in addition to this constant seasonally enhanced sediment supply, stadial fluctuations in the extent of the AIS injected extraordinary amounts of sediment into the Danube River (Martinez-Lamas et al., 2020). Recently, Baykal et al. (2022) showed that such proglacial sediment supply events caused episodic and intense dust fall along the Eurasian Ice Sheet meltwater drainage route based on chronological and provenance analyses of last glacial loess in SE England. However, the wider importance of this mechanism in controlling atmospheric dust loading and its impact on North Atlantic climate fluctuations during the LGP remains unexplored. Here we test the role of AIS-dynamics in driving abrupt changes in dust deposition across central Europe through multi-method source analysis (detrital zircon ages, heavy mineral assemblages, garnet chemistry and quartz grain morphology) of the previously high-sampling-resolution radiocarbon dated last glacial loess from Dunaszekcső (DSZ) in the Middle Danube Basin (Figure 1a).

2. Materials and Methods

2.1. Sampling Sites

Eight loess samples were taken from the Dunaszekcső loess section, located at the edge of a large loess plateau in southern Hungary (DSZ; Figure 1). Samples were selected from intervals with contrasting dust mass accumulation rates during 34–24 ka cal BP, derived from an existing 5-cm-resolution radiocarbon chronology (Újvári et al., 2014, 2017) (Figure 2c). Potential loess source samples were taken from modern Danube river sediments at Dunafalva (MDD) and Acs, Hungary (MDA), last glacial Danube river sediments at Acs (ACS-2), Holocene Drava and Tisza river sediments at Vejti, Hungary (DVM-3) and Ada, Serbia (TAM-3; see Figure 1 for locations), respectively, and Miocene-Pliocene fluvial sediments at five different locations near the Transdanubian Range (see Supporting Information S1 for details).

2.2. Detrital Zircon U–Pb Dating

Detrital zircons were extracted using density and magnetic separation and analyzed by LA-ICP-MS following standard procedures at the Arizona LaserChron Center (Gehrels et al., 2006, 2008; Pullen et al., 2018; see

10.1029/2025GL115382

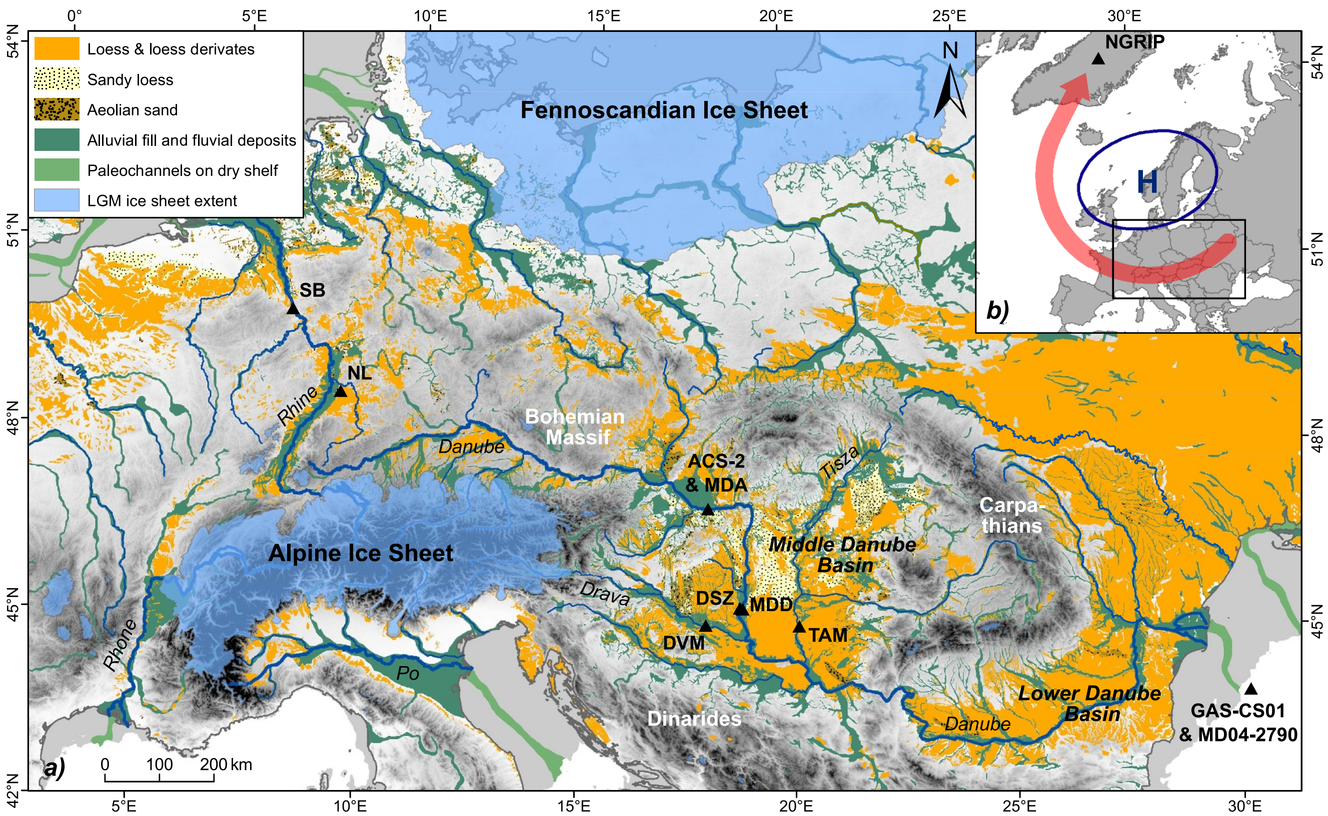

Figure 1. (a) Map of central Europe showing the distribution of loess and cover sands (Lehmkuhl et al., 2021) and LGM ice sheet extents modified from Ehlers et al. (2011). Location of Dunaszekcső loess section (DSZ), potential dust source sediment samples (MDD, MDA, ACS, DVM and TAM), other loess sections (NL, Nussloch; SB, Schwalbenberg) and Danube delta sediment cores in the Black Sea indicated by black triangles. (b) Inset map showing NGRIP site, proposed dominant LGM atmospheric circulation and Europe–Greenland dust trajectory based on Schaffernicht et al. (2020) and Újvári et al. (2022).

Supporting Information S1 for details). The "Best Age" was defined as $^{206}Pb/^{236}U$ age for analyses with $^{206}Pb/^{236}U$ age < 900 Ma and $^{206}Pb/^{207}Pb$ for analyses with $^{206}Pb/^{236}U$ age > 900 Ma. Concordance was based on $^{206}Pb/^{236}U$ age/$^{206}Pb/^{207}Pb$ age. This value was not reported for $^{206}Pb/^{236}U$ age < 400 Ma because of large uncertainty in the $^{206}Pb/^{207}Pb$ age. Age data with $^{206}Pb/^{236}U$ age > 400 Ma and with >20% discordance or >5% reverse discordance were not included in further analyses.

2.3. Heavy Mineral Assemblages

Heavy minerals were separated using Na-polytungstate (2.90 g/cm^3) from a split aliquot of the ∼7-ϕ-wide 5–500 μm size window obtained by wet sieving (Andò, 2020). On each grain mount, 200–250 transparent heavy minerals (tHM) were point-counted at suitable regular spacing to minimize overestimation of smaller grains. The identification of all silt-sized and dubious grains was validated using Raman spectroscopy. Based on tHM concentration (tHMC), tHM suites range from "poor" (tHMC < 1) to "moderately rich" (2 ≤ tHMC < 5) (Garzanti & Andò, 2019). Minerals are invariably listed in order of abundance.

2.4. Garnet Chemistry by Raman Spectroscopy

For obtaining the molar compositions of minerals of the garnet group, Raman spectroscopy was applied following Bersani et al. (2009) and using an unpublished updated version of this Matlab® routine (see Supporting Information S1 for details).

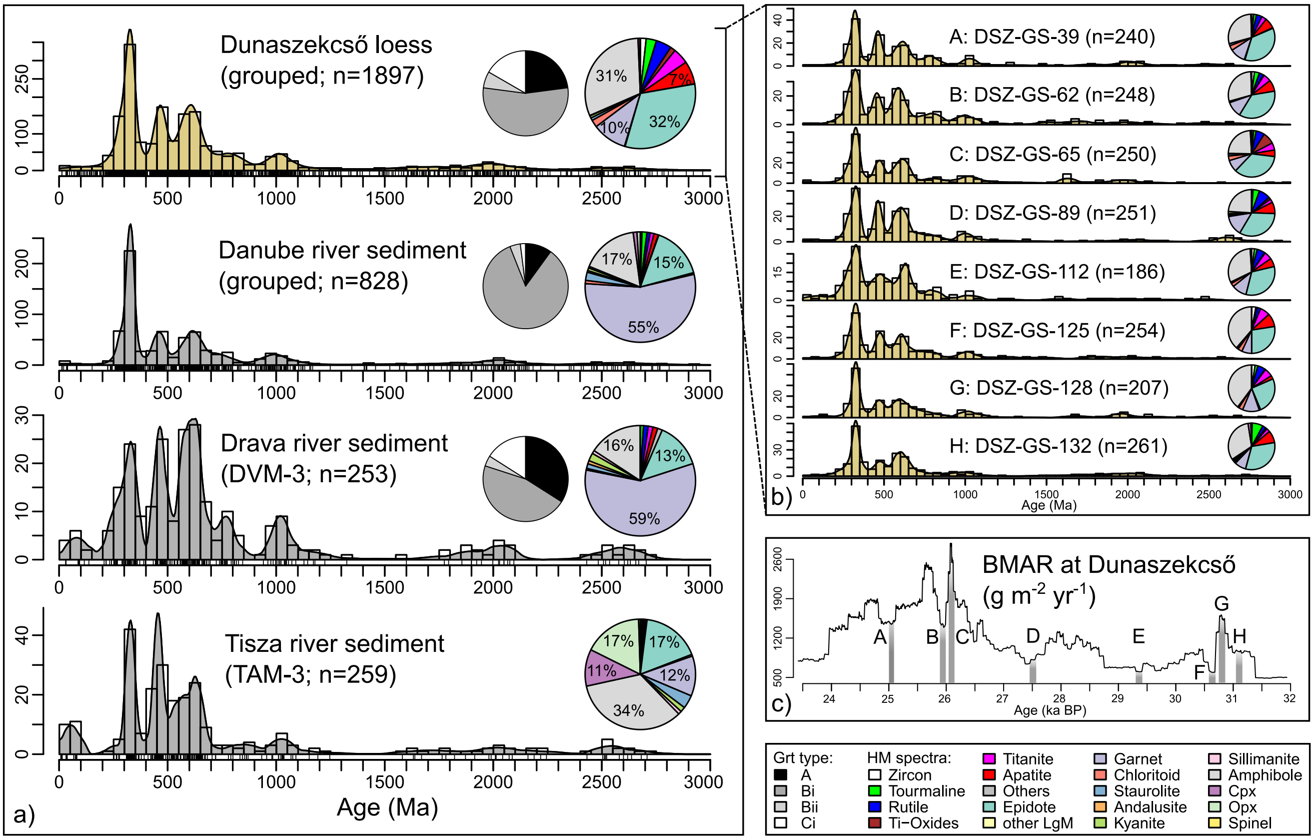

Figure 2. (a) KDE diagrams of detrital zircon U–Pb ages and pie charts of heavy minerals and garnet chemistry of DSZ loess and Danube river sediment (zircon and heavy mineral data grouped, garnet data from samples DSZ-89 and MDA, respectively) and Drava and Tisza river sediments. See Supporting Information S1. for garnet types. (b) Zircon age and heavy mineral spectra of individual loess samples from DSZ. (c) DSZ loess samples in relation to bulk mass accumulation rates (BMAR) (Újvári et al., 2017).

3. Results

3.1. Detrital Zircon U–Pb Dating

Detrital zircon U–Pb age distributions from all DSZ loess samples exhibit a dominant Carboniferous (~325 Ma) and subordinate Ordovician (~465 Ma) and late Neoproterozoic (~605 Ma) age peaks; Mesoproterozoic-Archean zircon ages are minor (Figure 2b). Age distributions from Danube samples MDD, MDA and ACS-2 are presented in the Figure S1 of Supporting Information S1. Age distributions of the grouped Danube, Drava (DVM-3) and Tisza (TAM-3) samples exhibit dominant Carboniferous (~325 Ma), Ordovician (~465 Ma) and late Neoproterozoic (~605 Ma) age peaks of varying relative importance alongside minor proportions of Mesoproterozoic-Archean age zircons (Figure 2a).

3.2. Heavy Mineral Assemblages

All DSZ loess samples yielded a moderately rich tHM suite with subequal epidote group minerals and amphibole (mostly blue-green hornblende and actinolite), associated with garnet, apatite, titanite, rutile, tourmaline, chloritoid, zircon, anatase, staurolite, kyanite and pyroxene (ZTR 6–14; Figure 2b). Heavy mineral spectra of individual Danube samples (MDD, MDA, ACS-2) and Miocene-Pliocene fluvial sands sampled near the Transdanubian Range are presented in the Supporting Information S1. The grouped Danube sample contains a moderately rich suite with mainly garnet, subordinate amphibole and epidote, and minor staurolite, pyroxene, tourmaline, apatite, titanite and chloritoid. Drava sample DVM-3 contains a quite similar, moderately rich suite with mainly garnet, subordinate amphibole and epidote, and minor kyanite, staurolite, apatite, titanite and rutile, whereas the moderately poor suite of Tisza sample TAM-3 contains amphibole, epidote, hypersthene, garnet, clinopyroxene, and minor staurolite, kyanite and sillimanite (Figure 2a).

3.3. Garnet Chemistry

A total of 368 garnet grains from 8 samples were analyzed and classified using the Mange and Morton (2007) scheme (Figure S4 in Supporting Information S1). The garnet chemical composition of the DSZ loess sample DSZ-GS-89, the Danube (MDA) and the Drava sample (DVM-3) primarily contain the garnet types Bi and A (Figure 2a) with almandine and spessartine as dominant endmembers (Figure S4 in Supporting Information S1). Garnet chemistry of Miocene-Pliocene fluvial sands sampled near the Transdanubian Range is presented in the Figure S3 of Supporting Information S1.

4. Discussion

4.1. Loess Sources in the Middle Danube Basin

All analyzed DSZ loess samples exhibit virtually identical zircon U–Pb age distributions and heavy mineral assemblages, indicating a constant source for loess deposition at DSZ during 32–24 ka (Figure 2c). This dust source will be inferred based on grouped detrital zircon U–Pb ages and heavy mineral suites of all analyzed DSZ loess samples (Figure 2a).

The grouped detrital zircon U–Pb age distribution of DSZ loess samples is dominated by three age peaks centered on ∼325, ∼465 and ∼605 Ma (Figure 2a). These ages reflect consecutive phases of widespread enhanced tectonism and magmatism in proto-source terranes associated with the Cadomian orogeny along the northern margin of Gondwana (670–510 Ma) (Linnemann et al., 2008), the closure of the Iapetus ocean and Caledonian orogeny (510–380 Ma) (McKerrow et al., 2000), and the collision between Laurussia and Gondwana resulting in the Variscan orogeny (380–280 Ma) (Stephan et al., 2019). Tectonic units of the Alpine-Carpathian-Dinaric system affected by these orogenic events represent the basement of today's Middle Danube Basin and are exposed in the surrounding mountain belts including the Alps and the Carpathians (Schmid et al., 2008) (Figure 1a). Cadomian, Caledonian and Variscan age zircon grains are thus widespread in sediments of rivers that drain these mountain regions, including the Danube, the Drava and the Tisza (Ducea et al., 2018; Fenn et al., 2022) (Figure 2a), all representing potential sources for loess at DSZ.

Based on the relative importance of the dominant zircon age components, Danube river sediments tend to match the loess best with a most important Variscan and similarly less important Caledonian and Cadomian zircon age peaks (Figure 2a). Qualitative differences in heavy mineral compositions facilitate a more robust discrimination between the river sediment provenances. While the Danube and Drava samples exhibit heavy mineral suites typically associated with a metamorphic orogenic source dominated by garnet, amphibole and epidote (Andò et al., 2014) (Figure 2a), the Tisza suite largely includes Ti-rich amphibole, augite and hypersthene potentially sourced from abundant calc-alkaline volcanic rocks in the Carpathians (Ducea et al., 2018; Schmid et al., 2008). Low ZTR values (≤3) in all fluvial sediment samples indicate that heavy mineral suites are largely unaffected by post-depositional weathering and dissolution processes (Garzanti, 2017) and thus reflect original detrital assemblages.

A direct comparison between heavy mineral suites of fluvial sediment and DSZ loess samples fails to provide a perfect match. The rarity of pyroxenes and magmatic amphiboles in the loess clearly rules out Tisza sediments as a major loess source. The orogenic suite of Danube and Drava sediments fits the qualitative composition of the loess, although loess samples have less garnet and more epidote and amphibole (Figure 2a). However, these quantitative differences in heavy mineral spectra of fluvial and aeolian sediments may result from grain size and sorting effects during transport. Sand transported as bedload in rivers is expected to be notably enriched in denser minerals such as garnet, whereas epidote typically concentrates in the suspended load (Garzanti, Andò, et al., 2010, 2011). The epidote/garnet ratio, and thus the similarity with the heavy mineral suite in DSZ loess, is in fact observed to notably increase from medium to fine and very fine Danube sand (unpublished data), as well as in very fine sand and silt classes of Drava sediments (Garzanti et al., 2008). When deflated and transported in atmospheric suspension, gravitational sorting would shift the sediment composition even further toward less-dense minerals. If such grain-size and sorting effects are taken into account, the heavy mineral signatures of Danube and Drava sediments can be reconciled well with the signature of the DSZ loess.

While the Drava only drains the Eastern Alps, the Danube catchment upstream from DSZ also includes smaller mountain regions such as the Bohemian Massif or the Transdanubian Range, and previous research has been divided over which of these terranes has been more efficient in silt production for regional loess deposition

(Buggle et al., 2008; Fenn et al., 2022; Újvári et al., 2013; Újvári & Klötzli, 2015). Heavy mineral analysis of loess at DSZ reveals significant amounts of chloritoid (Figure 2a), which is relatively uncommon in modern sediments. Yet, chloritoid occurs in low-grade Alpine metapelites (e.g., the Buendnerschiefer) exposed in the Tauern and Rechnitz tectonic windows in the eastern Alps drained by several Danube (sub)tributaries (Garzanti, Resentini, et al., 2010), and is thus also found in small amounts in Danube sediment samples. This Alpine provenance is also consistent with the chemical composition of garnets in the loess, including greenschist- (solid solution of Alm-Sps-Grs) and amphibolite-facies derived garnets (Alm-Prp) along with grains derived from magmatic rocks (Alm-Sps) (Figure 2a; Figure S4 in Supporting Information S1). Finally, previous detrital zircon Hf isotope analyses of loess nearby DSZ found signatures that also overlap with Austroalpine basement exposed in the Tauern Window (Fenn et al., 2022), all suggesting an Eastern Alpine proto-source contribution to loess in the Middle Danube Basin.

During the LGM, the Eastern Alps were covered by the extensive AIS and basement rocks would have been subjected to intense erosion by local ice streams. Glacially ground sediment particles would have been released along with glacial meltwater into proglacial river systems, that is, the Drava and Danube (Martinez-Lamas et al., 2020) and floodplain deposits may have subsequently acted as a widespread source for dust deflation and loess deposition. This model of loess genesis is also reflected in the morphology of quartz grains from DSZ loess (Figure S5 in Supporting Information S1): angular, sharp-edged grains with abundant high-pressure induced fracture marks are specific to subglacial grinding processes whereas V-shaped percussion marks result from grain collisions during high-energy fluvial transport (i.e., subglacial or proglacial meltwater flooding) (Baykal et al., 2022; Mahaney, 1995; Strand et al., 2003). As such, our multi-method provenance data from loess at DSZ presents a comprehensive picture of particle production in previously glaciated areas in the Eastern Alps and transport via the proglacial Danube river (and tributaries) prior to dust deflation from floodplain sediments. Previously proposed contributions from more local dust sources (e.g., smaller river systems or local cover sediments) are considered to be negligible for loess deposition at DSZ (see Section S2 in Supporting Information S1 for further discussion). Instead, our data indicate that AIS-derived sediments transported via the Danube river system acted as dominant and temporally stable dust source for loess deposition at DSZ throughout the late LGP.

4.2. Alpine Ice Sheet Dynamics Drive Stadial Dust Activity

Establishing that AIS-derived sediments, routed via the Danube river system, were the main source for loess in the Middle Danube Basin raises the key question as to how Quaternary AIS-dynamics affected dust sources and, by extension, loess deposition and atmospheric dust activity. In fact, it has been proposed that the onset of loess accumulation in the Danube basin was directly associated with the initial formation of significant ice caps in the Alps during the Mid-Pleistocene Transition, reinforcing the fundamental importance of glacial silt production and supply for regional loess formation (Obreht et al., 2019). This link between Alpine glaciation and peri-Alpine loess deposition is also observed on shorter, glacial-interglacial and subglacial timescales (Marković et al., 2024). Grouped luminescence data and derived accumulation rates from loess in the Middle Danube Basin and other regions surrounding the Alps indicate greatly enhanced dust deposition during the AIS advances of MIS 4 and, most significantly, MIS 2 (Bosq et al., 2023; Perić et al., 2022). Despite this, the role of the AIS in driving millennial-scale changes in last glacial dust activity as recorded in loess from DSZ (Figure 3c) remains unexplored.

The last glacial AIS is estimated to have reached its maximum extent at 25–24 ka, however, both the advance and retreat from this area were highly dynamic (Seguinot et al., 2018). Specifically, stadial cold periods were associated with wider recession of the AIS which contrasts the common expectation that continental ice sheets would expand during cold periods and shrink during warmer periods, if precipitation is constant (Martinez-Lamas et al., 2020). The causes for this counterintuitive behavior of the AIS remain debated but it is likely that large-scale atmospheric reorganizations during North Atlantic cooling caused summertime warming in Europe resulting in enhanced seasonality and surface melting of the AIS (Boswell et al., 2019; Martinez-Lamas et al., 2020). Large parts of the northeastern AIS lie within the Danube catchment and stadial ice sheet recession of this sector repeatedly unleashed summertime meltwater floods during the late LGP (Figure 3f). Along with glacial floodwaters, large volumes of glacigenic sediments were introduced to the Danube river system, as reflected by abrupt increases of sediment accumulation rates in the Danube delta (Martinez-Lamas et al., 2020) (Figures 3d and 3e). When glacial meltwater production seasonally ceased, these sediments were exposed in floodplains, turning the entire Danube river system into an efficient although intermittent source for dust deflation

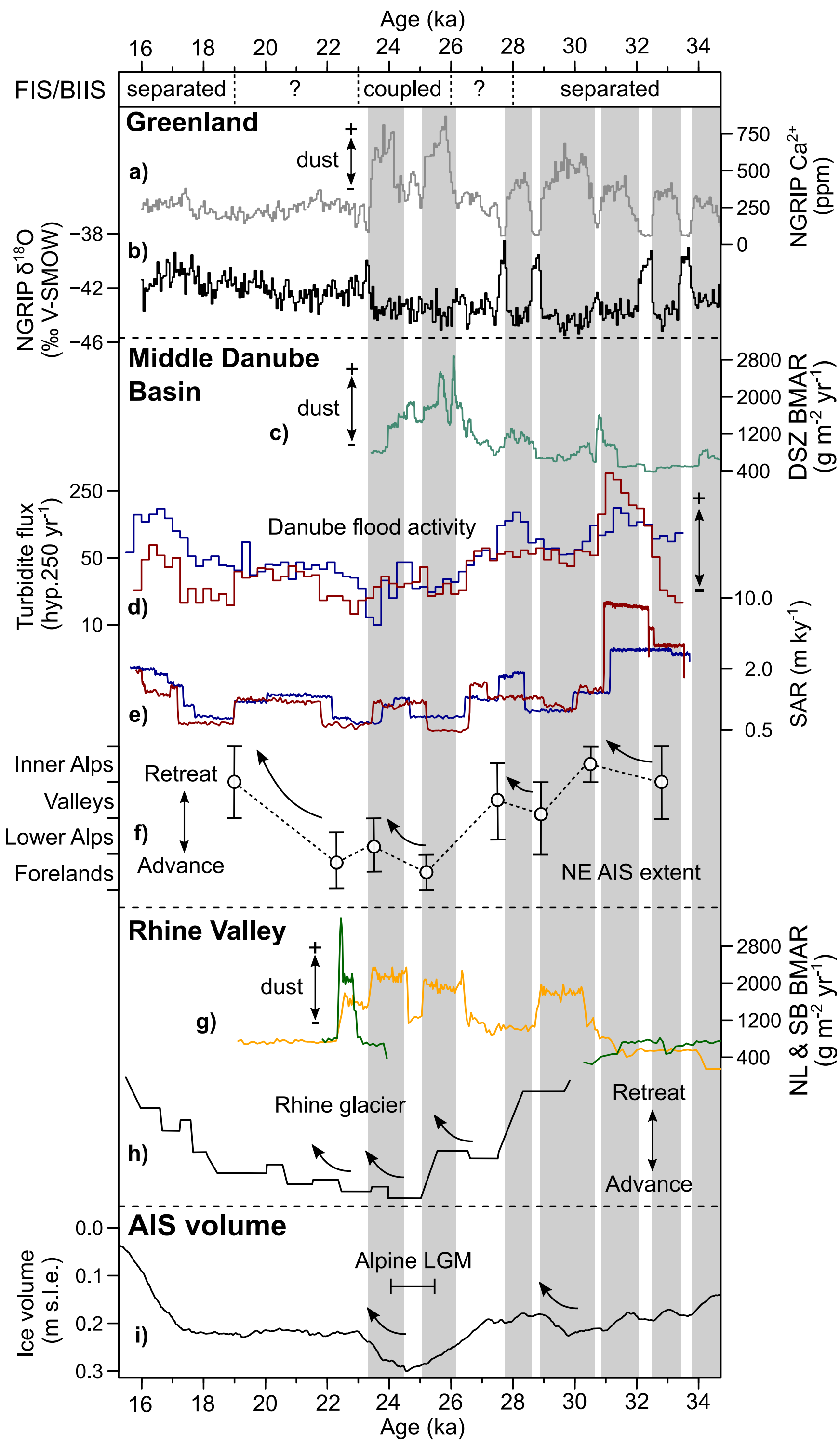

Figure 3. (a) NGRIP dust particle concentration and (b) $\delta^{18}O$ data (Rasmussen et al., 2014). (c) BMAR from DSZ loess (Újvári et al., 2017). (d) Turbidite flux and (e) sediment accumulation rates (SAR) from Danube delta sediment cores (Martinez-Lamas et al., 2020). (f) NE AIS extent based on Danube delta sediment provenance and SAR (Martinez-Lamas et al., 2020). (g) BMAR from loess at Nussloch (NL; orange) and Schwalbenberg (SB; green) (Fischer et al., 2021; Moine et al., 2017; Prud'homme et al., 2022). (h) Chronology of Rhine glacier advance and retreat dynamics (Preusser et al., 2011). (i) Modeled AIS volume (Seguinot et al., 2018). Gray bars indicate elevated NGRIP dust particle concentrations during stadials. Black arrows indicate glacier/ice sheet retreats. Timing of Fennoscandian (FIS) and British-Irish Ice Sheet (BIIS) coalescence in central North Sea noted at top (based on (Clark et al., 2022; Roberts et al., 2018; Sejrup et al., 2016)).

and loess deposition. Indeed, the timing of these AIS-driven sediment supply events overlaps with detected periods of greatly accelerated stadial dust deposition at DSZ during 32–24 ka BP (Újvári et al., 2017) (Figure 3c). Based on these close temporal links alongside our provenance data showing that DSZ loess is sourced from AIS-derived sediments, we propose that millennial-scale dust deposition variability at DSZ was mainly controlled by AIS-driven sediment supply. We also propose that this is a widespread effect. Extensive single grain and bulk sediment provenance studies of loess from the Middle and Lower Danube Basins demonstrate that Danube floodplain sediments represented the dominant source for wider loess deposition, with no major changes in source signature along the river (Fenn et al., 2022, 2025; Pötter et al., 2021). Furthermore, thorough morphological studies of quartz grains in loess found that glacially produced particles generally predominate in the Middle and Lower Danube Basins (Banak et al., 2013; Jordanova & Jordanova, 2024), all suggesting that stadial AIS-driven meltwater pulses and associated sediment supply caused widespread and intense dust fall episodes along the Danube River during the LGP.

Beyond the Danube basin, other major river systems such as the Po, the Rhône and the Rhine were affected by meltwater pulses derived from western and southern sectors of the last glacial AIS (Figure 1). Provenance studies of the extensive loess cover from these river basins also increasingly identify AIS-derived sediments as the main regional loess source (Bosq, Bertran, et al., 2020; Costantini et al., 2018; Zerboni et al., 2015). Moreover, generally enhanced late last glacial dust accumulation reported from this peri-Alpine loess (Bosq, Kreutzer, et al., 2020; Wacha et al., 2018) indicates that increased glacigenic sediment supply from the advanced AIS may have enhanced dust activity also across these regions. Indeed, more detailed chronological study of loess in the Rhine valley revealed substantial dust deposition variability during the late LGP (Fischer et al., 2021; Moine et al., 2017), with phases of enhanced dust activity that overlap with stadial AIS recession phases and, more specifically, retreats of the Rhine glacier (Figures 3g–3i). As such, late last glacial dust deposition variability widely seen in peri-Alpine loess seems to be a function of AIS-driven sediment supply. The timing of AIS-driven dust activity in the Rhine Valley and the Middle Danube Basin appears to be synchronized during the Alpine LGM. Offsets in the timing of dust fall episodes prior to the LGM may have been caused by regional differences in the timing of ice sheet recession or by temporary glacial lakes in the Alpine foreland that buffered meltwater pulses and trapped meltwater sediment (Martinez-Lamas et al., 2020). As such, AIS-driven meltwater pulses and associated sediment supply greatly enhanced atmospheric dust loading over Europe during stadial periods of the LGP.

4.3. Wider Dispersal of Ice Sheet Dust and the Climate Impact

Notably, the timing of AIS-driven dust events in the Middle Danube Basin and the Rhine Valley overlaps with stadial dust peaks reported from last glacial Greenland ice cores (Rasmussen et al., 2014) (Figure 3a). This coupled European-Greenland dust activity may reflect wider dispersal of AIS-derived dust particles to source distal locations in the North Atlantic region. Empirical evidence for Greenland dust provenance remains ambiguous, yet overlapping isotopic signatures of LGM Greenland dust and central European loess raise the possibility for a European dust source contribution (Újvári et al., 2015, 2022). In fact, regional climate models suggest that dominant anticyclonic circulation over the Eurasian Ice Sheet during the LGM offered efficient dust trajectories from Europe to Greenland (Újvári et al., 2022) (Figure 1b). The extent and strength of this high-pressure system would have been controlled by the size of the Eurasian Ice Sheet (Krinner et al., 2004; Ludwig et al., 2016; Schaffernicht et al., 2020). Specifically, coalescence of the British-Irish and Fennoscandian Ice Sheets in the central North Sea may have strengthened and caused a westward expansion of the high-pressure cell (Stevens et al., 2020). The exact timing of this ice sheet coalescence is uncertain, yet recent ice sheet chronologies agree that coupling of the British-Irish and Fennoscandian Ice Sheets at least lasted from 26 to 23 ka (Clark et al., 2022; Patton et al., 2017; Roberts et al., 2018) (Figure 3). Dust cycle simulations suggest that anticyclonic circulation and associated east-sector winds prevailed over central Europe 36% of the time under this ice sheet configuration (Schaffernicht et al., 2020), likely contributing to enhanced dust activity as reflected by peak loess accumulation rates reported from peri-Alpine loess during this interval (Bosq et al., 2023; Moine et al., 2017; Újvári et al., 2017) (Figures 3c and 3g). Strikingly, dust particle concentrations in Greenland ice cores also reach maximum values during 26–23 ka (Rasmussen et al., 2014) (Figure 3a), suggesting that strengthened anticyclonic circulation over northern Europe also enhanced wider atmospheric dispersal of AIS-derived dust particles across the North Atlantic region. In this way, AIS-driven dust events recorded in peri-Alpine loess would have altered atmospheric dust loading on continental-hemispheric scales during the LGP.

Such large-scale AIS-driven stadial dust events may also have modulated last glacial climate. Although the net effect is uncertain, atmospheric dust loading is most likely to have a moderate to substantial negative effect on the global radiation budget (Kok et al., 2023). By definition, AIS-driven dust outbreaks primarily affect ice marginal regions while wider atmospheric dust dispersal potentially reached North Atlantic high latitudes (Figure 1b). Across these cold climate regions, the cooling effect of dust in the atmosphere may be more significant, as the mixed-phase clouds formed around ice-nucleating dust particles affect radiation more efficiently (Shi et al., 2022; Shi & Liu, 2019). At the same time, a large proportion of dust emitted from regions marginal to the AIS is likely to be deposited on ice, both locally in the Alps and potentially more widely in the North Atlantic region. Dust on ice reduces albedo and accelerates ice melt rates resulting in enhanced ice sheet decay (Lamare et al., 2016; Oerlemans et al., 2009). In this way, AIS-driven dust activity during stadials may act to further cool climate, but at the same time contribute to enhanced ice sheet decay. This complex climate forcing impact of AIS-driven dust activity would thus perfectly augment the counterintuitive occurrence of synchronous climate cooling and enhanced ice sheet calving activity in central Europe (AIS) and the wider North Atlantic region during Greenland stadials and, most pronounced, Heinrich stadials of the LGP. As such, we propose that stadial AIS meltwater pulses amplified last glacial North Atlantic climate fluctuations via their impact on the mineral dust cycle. This previously unrecognized mechanism adds a new dimension to LGP rapid climate change events and urgently needs to be addressed in the modeling of last glacial climate evolution.

Conflict of Interest

The authors declare no conflicts of interest relevant to this study.

Data Availability Statement

All new provenance data from windblown dust (loess) and fluvial sediments from the Middle Danube Basin (central Europe) have been archived at Zenodo (Baykal et al., 2025).

Acknowledgments

Chiara Költringer is thanked for her help during the fieldwork, Pietro Caruso for measuring Raman spectra of garnets, Danilo Bersani for providing the updated version of the Matlab routine "MIRAGEM", Gábor Csillag and Krisztina Sebe for their help with finding sampling locations of Miocene-Pliocene Pannonian deposits, and reviewers Slobodan Marković and Junsheng Nie for constructive feedback that significantly improved this manuscript. This work was funded by the Swedish Research Council (VR Grant 2017-03888, TS), the Quaternary Research Association (QRA) Quaternary Research Fund and the Independent Research Fund Denmark (DFF Grant 10.46540/4283-00198B).

References

Andò, S. (2020). Gravimetric separation of heavy minerals in sediments and rocks. *Minerals*, *10*(3), 273. https://doi.org/10.3390/min10030273

Andò, S., Morton, A., & Garzanti, E. (2014). In *Metamorphic grade of source rocks revealed by chemical fingerprints of detrital amphibole and garnet* (Vol. 386, pp. 351–371). Geological Society Special Publication. https://doi.org/10.1144/SP386.5

Banak, A., Pavelić, D., Kovačić, M., & Mandic, O. (2013). Sedimentary characteristics and source of loess in Baranja (Eastern Croatia). *Aeolian Research*, *11*, 129–139. https://doi.org/10.1016/j.aeolia.2013.08.002

Baykal, Y., Stevens, T., Bateman, M. D., Pfaff, K., Sechi, D., Banak, A., et al. (2022). Eurasian Ice Sheet derived meltwater pulses and their role in driving atmospheric dust activity: Late Quaternary loess sources in SE England. *Quaternary Science Reviews*, *296*, 107804. https://doi.org/10.1016/j.quascirev.2022.107804

Baykal, Y., Stevens, T., Engström-Johansson, A., Skurzyński, J., Zhang, H., He, J., et al. (2021). Detrital zircon U–Pb age analysis of last glacial loess sources and proglacial sediment dynamics in the Northern European Plain. *Quaternary Science Reviews*, *274*, 107265. https://doi.org/10.1016/j.quascirev.2021.107265

Baykal, Y., Ujvari, G., Stevens, T., Andò, S., Banak, A., Šuica, S., et al. (2025). Provenance data from windblown dust (loess) and fluvial sediments from the Middle Danube Basin (central Europe) [Dataset]. *Zenodo*. https://doi.org/10.5281/zenodo.14883273

Bersani, D., Andò, S., Vignola, P., Moltifiori, G., Marino, I. G., Lottici, P. P., & Diella, V. (2009). Micro-Raman spectroscopy as a routine tool for garnet analysis. *Spectrochimica Acta, Part A: Molecular and Biomolecular Spectroscopy*, *73*(3), 484–491. https://doi.org/10.1016/j.saa.2008.11.033

Bosq, M., Bertran, P., Degeai, J. P., Queffelec, A., & Moine, O. (2020). Geochemical signature of sources, recycling and weathering in the Last Glacial loess from the Rhône Valley (Southeast France) and comparison with other European regions. *Aeolian Research*, *42*, 100561. https://doi.org/10.1016/j.aeolia.2019.100561

Bosq, M., Kreutzer, S., Bertran, P., Degeai, J. P., Dugas, P., Kadereit, A., et al. (2020). Chronostratigraphy of two late Pleistocene loess-Palaeosol sequences in the Rhône valley (Southeast France). *Quaternary Science Reviews*, *245*, 106473. https://doi.org/10.1016/j.quascirev.2020.106473

Bosq, M., Kreutzer, S., Bertran, P., Lanos, P., & Dufresne, P. (2023). Last glacial loess in Europe: Luminescence database and chronology of deposition. *Earth System Science Data, 7728616*, *15*, 1–31.

Boswell, S. M., Toucanne, S., Pitel-Roudaut, M., Creyts, T. T., Eynaud, F., & Bayon, G. (2019). Enhanced surface melting of the Fennoscandian ice sheet during periods of North Atlantic cooling. *Geology*, *47*(7), 664–668. https://doi.org/10.1130/G46370.1

Buggle, B., Glaser, B., Zöller, L., Hambach, U., Markovic, S., Glaser, I., & Gerasimenko, N. (2008). Geochemical characterization and origin of Southeastern and Eastern European loesses (Serbia, Romania, Ukraine). *Quaternary Science Reviews*, *27*(9–10), 1058–1075. https://doi.org/10.1016/j.quascirev.2008.01.018

Bullard, J. E., Baddock, M., Bradwell, T., Crusius, J., Darlington, E., Gaiero, D., et al. (2016). High-latitude dust in the Earth system. *Reviews of Geophysics*, *54*(2), 447–485. https://doi.org/10.1002/2016RG000518

Clark, C. D., Ely, J. C., Hindmarsh, R. C. A., Bradley, S., Eczi, A. I. G. N., Chiverrell, R. C., et al. (2022). Growth and retreat of the last British – Irish ice sheet, 31 000 to 15 000 years ago: The BRITICE-CHRONO reconstruction. *Boreas*, *51*(4), 699–758. https://doi.org/10.1111/bor.12594

Clark, P. U., Dyke, A. S., Shakun, J. D., Carlson, A. E., Clark, J., Wohlfarth, B., et al. (2009). The last glacial maximum. *Science*, *325*(5941), 710–714. https://doi.org/10.1126/science.1172873

Costantini, E. A. C., Carnicelli, S., Sauer, D., Priori, S., Andreetta, A., Kadereit, A., & Lorenzetti, R. (2018). Loess in Italy: Genesis, characteristics and occurrence. *Catena*, *168*, 14–33. https://doi.org/10.1016/j.catena.2018.02.002

Ducea, M. N., Giosan, L., Carter, A., Balica, C., Stoica, A. M., Roban, R. D., et al. (2018). U-Pb detrital zircon geochronology of the lower Danube and its tributaries; implications for the geology of the Carpathians. *Geochemistry, Geophysics, Geosystems*, *19*(9), 3208–3223. https://doi.org/10.1029/2018GC007659

Ehlers, J., Gibbard, P. L., & Hughes, P. D. (Eds.) (2011). *Quaternary glaciations-extent and chronology: A closer look* (Vol. 15). Elsevier.

Fenn, K., Millar, I. L., Bird, A., Veres, D., & Wagner, D. (2025). Provenance of late Pleistocene loess in central and Eastern Europe: Isotopic evidence for dominant local sediment sources. *Scientific Reports*, *15*(1), 1624. https://doi.org/10.1038/s41598-024-83698-5

Fenn, K., Millar, I. L., Durcan, J. A., Thomas, D. S. G., Banak, A., Marković, S. B., et al. (2022). The provenance of Danubian loess. *Earth-Science Reviews*, *226*, 103920. https://doi.org/10.1016/j.earscirev.2022.103920

Fischer, P., Jöris, O., Fitzsimmons, K. E., Vinnepand, M., Prud'homme, C., Schulte, P., et al. (2021). Millennial-scale terrestrial ecosystem responses to upper Pleistocene climatic changes: 4D-reconstruction of the Schwalbenberg loess-Palaeosol-sequence (Middle Rhine Valley, Germany). *Catena*, *196*, 104913. https://doi.org/10.1016/j.catena.2020.104913

Garzanti, E. (2017). The maturity myth in sedimentology and provenance analysis. *Journal of Sedimentary Research*, *87*(4), 353–365. https://doi.org/10.2110/jsr.2017.17

Garzanti, E., & Andò, S. (2019). Heavy minerals for junior woodchucks. *Minerals*, *9*(3), 148. https://doi.org/10.3390/min9030148

Garzanti, E., Andó, S., France-Lanord, C., Censi, P., Vignola, P., Galy, V., & Lupker, M. (2011). Mineralogical and chemical variability of fluvial sediments 2. Suspended-load silt (Ganga-Brahmaputra, Bangladesh). *Earth and Planetary Science Letters*, *302*(1–2), 107–120. https://doi.org/10.1016/j.epsl.2010.11.043

Garzanti, E., Andò, S., France-Lanord, C., Vezzoli, G., Censi, P., Galy, V., & Najman, Y. (2010b). Mineralogical and chemical variability of fluvial sediments. 1. Bedload sand (Ganga-Brahmaputra, Bangladesh). *Earth and Planetary Science Letters*, *299*(3–4), 368–381. https://doi.org/10.1016/j.epsl.2010.09.017

Garzanti, E., Andò, S., & Vezzoli, G. (2008). Settling equivalence of detrital minerals and grain-size dependence of sediment composition. *Earth and Planetary Science Letters*, *273*(1–2), 138–151. https://doi.org/10.1016/j.epsl.2008.06.020

Garzanti, E., Resentini, A., Vezzoli, G., Andò, S., Malusà, M. G., Padoan, M., & Paparella, P. (2010). Detrital fingerprints of fossil continental-subduction zones (Axial belt provenance, European Alps). *The Journal of Geology*, *118*(4), 341–362. https://doi.org/10.1086/652720

Gehrels, G., Valencia, V., & Pullen, A. (2006). Detrital zircon geochronology by laser-ablation multicollector ICPMS at the Arizona LaserChron Center. *Paleontological Society Papers*, *12*, 67–76. https://doi.org/10.1002/9781444347166.ch2

Gehrels, G. E., Valencia, V. A., & Ruiz, J. (2008). Enhanced precision, accuracy, efficiency, and spatial resolution of U–Pb ages by laser ablation-multicollector-inductively coupled plasma-mass spectrometry. *Geochemistry, Geophysics, Geosystems*, *9*(3). https://doi.org/10.1029/2007GC001805

Jordanova, D., & Jordanova, N. (2024). Geochemical and mineral magnetic footprints of provenance, weathering and pedogenesis of loess and Paleosols from North Bulgaria. *Catena*, *243*, 108131. https://doi.org/10.1016/j.catena.2024.108131

Kindler, P., Guillevic, M., Baumgartner, M., Schwander, J., Landais, A., & Leuenberger, M. (2014). Temperature reconstruction from 10 to 120 kyr b2k from the NGRIP ice core. *Climate of the Past*, *10*(2), 887–902. https://doi.org/10.5194/cp-10-887-2014

Kłapyta, P., Mîndrescu, M., & Zasadni, J. (2021). Geomorphological record and equilibrium line altitude of glaciers during the last glacial maximum in the Rodna Mountains (Eastern Carpathians). *Quaternary Research (United States)*, *100*, 1–20. https://doi.org/10.1017/qua.2020.90

Knippertz, P., & Stuut, J.-B. W. (2014). Mineral dust. https://doi.org/10.1007/978-94-017-8978-3

Kok, J. F., Storelvmo, T., Karydis, V. A., Adebiyi, A. A., Mahowald, N. M., Evan, A. T., et al. (2023). The impacts of mineral dust aerosols on global climate and climate change. *Nature Reviews Earth & Environment*, *4*(2), 71–86. https://doi.org/10.1038/s43017-022-00379-5

Krinner, G., Mangerud, J., Jakobsson, M., Crucifix, M., Ritz, C., & Svendsen, J. I. (2004). Enhanced ice sheet growth in Eurasia owing to adjacent ice-dammed lakes. *Nature*, *427*(6973), 429–432. https://doi.org/10.1038/nature02233

Lamare, M. L., Lee-Taylor, J., & King, M. D. (2016). The impact of atmospheric mineral aerosol deposition on the albedo of snow and sea ice: Are snow and sea ice optical properties more important than mineral aerosol optical properties? *Atmospheric Chemistry and Physics*, *16*(2), 843–860. https://doi.org/10.5194/acp-16-843-2016

Lehmkuhl, F., Nett, J. J., Pötter, S., Schulte, P., Sprafke, T., Jary, Z., et al. (2021). Loess landscapes of Europe – mapping, geomorphology, and zonal differentiation. *Earth-Science Reviews*, *215*, 103496. https://doi.org/10.1016/j.earscirev.2020.103496

Linnemann, U., Pereira, M. F., Jeffries, T. E., Drost, K., & Gerdes, A. (2008). The Cadomian orogeny and the opening of the Rheic ocean: The Diacrony of geotectonic processes constrained by LA-ICP-MS U–Pb zircon dating (Ossa-Morena and Saxo-Thuringian zones, Iberian and Bohemian Massifs). *Tectonophysics*, *461*(1–4), 21–43. https://doi.org/10.1016/j.tecto.2008.05.002

Ludwig, P., Schaffernicht, E. J., Shao, Y., & Pinto, J. G. (2016). Regional atmospheric circulation over Europe during the last glacial maximum and its links to precipitation. *Journal of Geophysical Research*, *121*(5), 2130–2145. https://doi.org/10.1002/2015JD024444

Mahaney, W. C. (1995). Glacial crushing, weathering and diagenetic histories of quartz grains inferred from scanning electron microscopy. In J. Menzies (Ed.), *Modern glacial environments—processes. Dynamics and sediments* (pp. 487–506). Butterworth-Heinemann Ltd.

Mange, M. A., & Morton, A. C. (2007). Geochemistry of heavy minerals. *Developments in Sedimentology*, *58*, 345–391. https://doi.org/10.1016/S0070-4571(07)58013-1

Marković, S. B., Hughes, P. D., Schaetzl, R., Gibbard, P. L., Hao, Q., Radaković, M. G., et al. (2024). The relationship between the loess stratigraphy in the Vojvodina region of northern Serbia and the Saalian and Rissian Stage glaciations–A review. *Boreas*, *53*(4), 577–592. https://doi.org/10.1111/bor.12646

Martinez-Lamas, R., Toucanne, S., Debret, M., Riboulot, V., Deloffre, J., Boissier, A., et al. (2020). Linking Danube River activity to alpine ice sheet fluctuations during the last glacial (ca. 33–17 ka BP): Insights into the continental signature of Heinrich Stadials. *Quaternary Science Reviews*, *229*, 106136. https://doi.org/10.1016/j.quascirev.2019.106136

McKerrow, W. S., Niocaill, C. M., & Dewey, J. F. (2000). The Caledonian orogeny redefined. *Journal of the Geological Society*, *157*(6), 1149–1154. https://doi.org/10.1144/jgs.157.6.1149

Mentlík, P., Engel, Z., Braucher, R., Léanni, L., Arnold, M., Aumaître, G., et al. (2013). Chronology of the late Weichselian glaciation in the Bohemian forest in central Europe. *Quaternary Science Reviews*, *65*, 120–128. https://doi.org/10.1016/j.quascirev.2013.01.020

Moine, O., Antoine, P., Hatté, C., Landais, A., Mathieu, J., Prud'homme, C., & Rousseau, D.-D. (2017). The impact of last glacial climate variability in West-European loess revealed by radiocarbon dating of fossil earthworm granules. *Proceedings of the National Academy of Sciences*, *114*(24), 6209–6214. https://doi.org/10.1073/pnas.1614751114

Obreht, I., Zeeden, C., Hambach, U., Veres, D., Marković, S. B., & Lehmkuhl, F. (2019). A critical reevaluation of palaeoclimate proxy records from loess in the Carpathian Basin. *Earth-Science Reviews*, *190*, 498–520. https://doi.org/10.1016/j.earscirev.2019.01.020

Oerlemans, J., Giesen, R. H., & Van Den Broeke, M. R. (2009). Retreating alpine glaciers: Increased melt rates due to accumulation of dust (Vadret da Morteratsch, Switzerland). *Journal of Glaciology*, *55*(192), 729–736. https://doi.org/10.3189/002214309789470969

Patton, H., Hubbard, A., Andreassen, K., Auriac, A., Whitehouse, P. L., Stroeven, A. P., et al. (2017). Deglaciation of the Eurasian ice sheet complex. *Quaternary Science Reviews*, *169*, 148–172. https://doi.org/10.1016/j.quascirev.2017.05.019

Perić, Z. M., Stevens, T., Obreht, I., Hambach, U., Lehmkuhl, F., & Marković, S. B. (2022). Detailed luminescence dating of dust mass accumulation rates over the last two glacial-interglacial cycles from the Irig loess-Palaeosol sequence, Carpathian Basin. *Global and Planetary Change*, *215*, 103895. https://doi.org/10.1016/j.gloplacha.2022.103895

Pötter, S., Veres, D., Baykal, Y., Nett, J. J., Schulte, P., Hambach, U., & Lehmkuhl, F. (2021). Disentangling sedimentary pathways for the Pleniglacial lower Danube loess based on Geochemical signatures. *Frontiers in Earth Science*, *9*. https://doi.org/10.3389/feart.2021.600010

Preusser, F., Graf, H. R., Keller, O., Krayss, E., & Schlüchter, C. (2011). Quaternary glaciation history of Northern Switzerland. *E&G Quaternary Science Journal*, *60*(2/3), 282–305. https://doi.org/10.3285/eg.60.2-3.06

Prud'homme, C., Fischer, P., Jöris, O., Gromov, S., Vinnepand, M., Hatté, C., et al. (2022). Millennial-timescale quantitative estimates of climate dynamics in central Europe from earthworm calcite granules in loess deposits. *Communications Earth & Environment*, *3*(1), 267. https://doi.org/10.1038/s43247-022-00595-3

Pullen, A., Ibáñez-Mejia, M., Gehrels, G. E., Giesler, D., & Pecha, M. (2018). Optimization of a laser ablation-single collector-inductively coupled plasma-mass spectrometer (Thermo element 2) for accurate, precise, and efficient zircon U-Th-Pb geochronology. *Geochemistry, Geophysics, Geosystems*, *19*(10), 3689–3705. https://doi.org/10.1029/2018GC007889

Rasmussen, S. O., Bigler, M., Blockley, S. P., Blunier, T., Buchardt, S. L., Clausen, H. B., et al. (2014). A stratigraphic framework for abrupt climatic changes during the last glacial period based on three synchronized Greenland ice-core records: Refining and extending the INTIMATE event stratigraphy. *Quaternary Science Reviews*, *106*, 14–28. https://doi.org/10.1016/j.quascirev.2014.09.007

Roberts, D. H., Evans, D. J. A., Callard, S. L., Clark, C. D., Bateman, M. D., Medialdea, A., et al. (2018). Ice marginal dynamics of the last British-Irish ice sheet in the southern North Sea: Ice limits, timing and the influence of the Dogger bank. *Quaternary Science Reviews*, *198*, 181–207. https://doi.org/10.1016/j.quascirev.2018.08.010

Ruth, U., Wagenbach, D., & Bigler, M. (2003). Continuous record of microparticle concentration and size distribution in the central Greenland NGRIP ice core during the last glacial period. *Journal of Geophysical Research*, *108*(D3), 1–12. https://doi.org/10.1029/2002JD002376

Schaffernicht, E. J., Ludwig, P., & Shao, Y. (2020). Linkage between dust cycle and loess of the last glacial maximum in Europe. *Atmospheric Chemistry and Physics*, *20*(8), 4969–4986. https://doi.org/10.5194/acp-2019-693

Schmid, S. M., Bernoulli, D., Fügenschuh, B., Matenco, L., Schefer, S., Schuster, R., et al. (2008). The Alpine-Carpathian-Dinaridic orogenic system: Correlation and evolution of tectonic units. *Swiss Journal of Geosciences*, *101*(1), 139–183. https://doi.org/10.1007/s00015-008-1247-3

Seguinot, J., Ivy-Ochs, S., Jouvet, G., Huss, M., Funk, M., & Preusser, F. (2018). Modelling last glacial cycle ice dynamics in the Alps. *The Cryosphere*, *12*(10), 3265–3285. https://doi.org/10.5194/tc-12-3265-2018

Sejrup, H. P., Clark, C. D., & Hjelstuen, B. O. (2016). Rapid ice sheet retreat triggered by ice stream debuttressing: Evidence from the North Sea. *Geology*, *44*(5), 355–358. https://doi.org/10.1130/G37652.1

Shi, Y., & Liu, X. (2019). Dust radiative effects on climate by glaciating mixed-phase clouds. *Geophysical Research Letters*, *46*(11), 6128–6137. https://doi.org/10.1029/2019GL082504

Shi, Y., Liu, X., Wu, M., Zhao, X., Ke, Z., & Brown, H. (2022). Relative importance of high-latitude local and long-range-transported dust for Arctic ice-nucleating particles and impacts on Arctic mixed-phase clouds. *Atmospheric Chemistry and Physics*, *22*(4), 2909–2935. https://doi.org/10.5194/acp-22-2909-2022

Smalley, I., Hara-dhand, K. O., Wint, J., Machalett, B., Jary, Z., & Jefferson, I. (2009). Rivers and loess: The significance of long river transportation in the complex event-sequence approach to loess deposit formation. *Quaternary International*, *198*(1–2), 7–18. https://doi.org/10.1016/j.quaint.2008.06.009

Smalley, I. J., & Leach, J. A. (1978). The origin and distribution of the loess in the Danube basin and associated regions of East-Central Europe—a review. *Sedimentary Geology*, *21*, 1–26. https://doi.org/10.1016/0037-0738(78)90031-3

Stephan, T., Kroner, U., Romer, R. L., & Rösel, D. (2019). From a bipartite Gondwanan shelf to an arcuate Variscan belt: The early Paleozoic evolution of northern Peri-Gondwana. *Earth-Science Reviews*, *192*, 491–512. https://doi.org/10.1016/j.earscirev.2019.03.012

Stevens, T., Sechi, D., Bradák, B., Orbe, R., Baykal, Y., Cossu, G., et al. (2020). Abrupt last glacial dust fall over southeast England associated with dynamics of the British-Irish ice sheet. *Quaternary Science Reviews*, *250*, 106641. https://doi.org/10.1016/j.quascirev.2020.106641

Strand, K., Passchier, S., & Näsi, J. (2003). Implications of quartz grain microtextures for onset Eocene/Oligocene glaciation in Prydz Bay, ODP site 1166, Antarctica. *Palaeogeography, Palaeoclimatology, Palaeoecology*, *198*(1–2), 101–111. https://doi.org/10.1016/S0031-0182(03)00396-1

Stuut, J. B., Smalley, I., & O'Hara-Dhand, K. (2009). Aeolian dust in Europe: African sources and European deposits. *Quaternary International*, *198*(1–2), 234–245. https://doi.org/10.1016/j.quaint.2008.10.007

Thamó-Bozsó, E., Kovács, L. Ó., Magyari, Á., & Marsi, I. (2014). Tracing the origin of loess in Hungary with the help of heavy mineral composition data. *Quaternary International*, *319*, 11–21. https://doi.org/10.1016/j.quaint.2013.04.030

Újvári, G., & Klötzli, U. (2015). U–Pb ages and Hf isotopic composition of zircons in Austrian last glacial loess: Constraints on heavy mineral sources and sediment transport pathways. *International Journal of Earth Sciences*, *104*(5), 1365–1385. https://doi.org/10.1007/s00531-014-1139-x

Újvári, G., Klötzli, U., Kiraly, F., & Ntaflos, T. (2013). Towards identifying the origin of metamorphic components in Austrian loess: Insights from detrital rutile chemistry, thermometry and U–Pb geochronology. *Quaternary Science Reviews*, *75*, 132–142. https://doi.org/10.1016/j.quascirev.2013.06.002

Újvári, G., Klötzli, U., Stevens, T., Svensson, A., Ludwig, P., Vennemann, T., et al. (2022). Greenland ice core record of last glacial dust sources and atmospheric circulation. *Journal of Geophysical Research: Atmospheres*, *127*(15). https://doi.org/10.1029/2022JD036597

Újvári, G., Molnár, M., Novothny, Á., Páll-Gergely, B., Kovács, J., & Várhegyi, A. (2014). AMS14C and OSL/IRSL dating of the Dunaszekcső loess sequence (Hungary): Chronology for 20 to 150ka and implications for establishing reliable age-depth models for the last 40ka. *Quaternary Science Reviews*, *106*, 140–154. https://doi.org/10.1016/j.quascirev.2014.06.009

Újvári, G., Stevens, T., Molnár, M., Demény, A., Lambert, F., Varga, G., et al. (2017). Coupled European and Greenland last glacial dust activity driven by North Atlantic climate. *Proceedings of the National Academy of Sciences*, *114*(50), E10632–E10638. https://doi.org/10.1073/pnas.1712651114

Újvári, G., Stevens, T., Svensson, A., Klötzli, U. S., Manning, C., Németh, T., et al. (2015). Two possible source regions for central Greenland last glacial dust. *Geophysical Research Letters*, *42*(23), 10399–10408. https://doi.org/10.1002/2015GL066153

Újvári, G., Varga, A., Ramos, F. C., Kovács, J., Németh, T., & Stevens, T. (2012). Evaluating the use of clay mineralogy, Sr-Nd isotopes and zircon U–Pb ages in tracking dust provenance: An example from loess of the Carpathian Basin. *Chemical Geology*, *304–305*, 83–96. https://doi.org/10.1016/j.chemgeo.2012.02.007

Urdea, P., Onaca, A., Ardelean, F., & Ardelean, M. (2011). New evidence on the quaternary glaciation in the Romanian Carpathians. *Developments in Quaternary Science*, *15*, 305–322. https://doi.org/10.1016/B978-0-444-53447-7.00024-6

Varga, G., Cserháti, C., Kovács, J., & Szalai, Z. (2016). Saharan dust deposition in the Carpathian Basin and its possible effects on interglacial soil formation. *Aeolian Research*, *22*, 1–12. https://doi.org/10.1016/j.aeolia.2016.05.004

Wacha, L., Rolf, C., Hambach, U., Frechen, M., Galović, L., & Duchoslav, M. (2018). The Last Glacial Aeolian record of the Island of Susak (Croatia) as seen from a high-resolution grain-size and rock magnetic analysis. *Quaternary International*, *494*, 211–224. https://doi.org/10.1016/j.quaint.2017.08.016

Zerboni, A., Trombino, L., Frigerio, C., Livio, F., Berlusconi, A., Michetti, A. M., et al. (2015). The loess-Paleosol sequence at Monte Netto: A record of climate change in the upper Pleistocene of the central Po plain, Northern Italy. *Journal of Soils and Sediments*, *15*(6), 1329–1350. https://doi.org/10.1007/s11368-014-0932-2

References From the Supporting Information

Black, L. P., Kamo, S. L., Williams, I. S., Mundil, R., Davis, D. W., Korsch, R. J., & Foudoulis, C. (2003). The application of SHRIMP to Phanerozoic geochronology; a critical appraisal of four zircon standards. *Chemical Geology*, *200*(1–2), 171–188. https://doi.org/10.1016/S0009-2541(03)00166-9

Black, L. P., Kamo, S. L., Allen, C. M., Davis, D. W., Aleinikoff, J. N., Valley, J. W., et al. (2004). Improved $^{206}Pb/^{238}U$ microprobe geochronology by the monitoring of a trace-element-related matrix effect; SHRIMP, ID-TIMS, ELA-ICP-MS and oxygen isotope documentation for a series of zircon standards. *Chemical Geology*, *205*(1–2), 115–140. https://doi.org/10.1016/j.chemgeo.2004.01.003

Magyar, I., Geary, D. H., & Müller, P. (1999). Paleogeographic evolution of the late Miocene lake Pannon in central Europe. *Palaeogeography, Palaeoclimatology, Palaeoecology*, *147*(3–4), 151–167. https://doi.org/10.1016/S0031-0182(98)00155-2

Mahaney, W. C. (2002). *Atlas of sand grain surface textures and applications* (Vol. 237). Oxford University Press.

Morton, A. C., & Hallsworth, C. (2007). Stability of detrital heavy minerals during Burial diagenesis. *Developments in Sedimentology*, *58*, 215–245. https://doi.org/10.1016/S0070-4571(07)58007-6

Nagy, A., Thamo, E., & Musitz, B. (2010). OSL ages and origin of late quaternary sediments in the North Transdanubian Hills (Hungary): Timing of neotectonic activity. *Quaternary International*, *222*(1–2), 209–220. https://doi.org/10.1016/j.quaint.2009.07.023

Pullen, A., Ibáñez-Mejía, M., Gehrels, G. E., Ibáñez-Mejía, J. C., & Pecha, M. (2014). What happens when n= 1000? Creating large-n geochronological datasets with LA-ICP-MS for geologic investigations. *Journal of Analytical Atomic Spectrometry*, *29*, 971–980. https://doi.org/10.1039/c4ja00024b

Sebe, K., Csillag, G., Fodor, L., Thamó-bozsó, E., Thamó-Bozsó, E., Müller, P., & Braucher, R. (2011). Wind erosion under cold climate: A Pleistocene periglacial Mega-Yardang system in central Europe (Western Pannonian Basin, Hungary). *Geomorphology*, *134*(3–4), 470–482. https://doi.org/10.1016/j.geomorph.2011.08.003